J|A|C|S
ARTICLES
Published on Web 11/08/2006

Cation Exchange in Lipophilic G-Quadruplexes: Not All Ion Binding Sites Are Equal

Ling Ma, Maura Iezzi, Mark S. Kaucher, Yiu-Fai Lam, and Jeffery T. Davis*

Contribution from the Department of Chemistry and Biochemistry, University of Maryland, College Park, Maryland 20742

Received July 9, 2006; E-mail: jdavis@umd.edu

Abstract: Lipophilic guanosine derivatives that form G-quadruplexes are promising building blocks for ionophores and ion channels. Herein, cation exchange between solvated cations (K^+ and NH_4^+) and bound cations in the G-quadruplex $[G\mathbf{1}]_{16}\cdot 4Na^+\cdot 4DNP^-$ was studied by electrospray ionization mass spectrometry and solution ^1H, ^{15}N NMR spectroscopy. The ESI-MS and ^1H NMR data provided evidence for the formation of mixed-cationic Na^+, K^+ G-quadruplexes. The use of $^{15}NH_4^+$ cations in NMR titrations, along with ^{15}N-filtered ^1H NMR and selective NOE experiments, identified two mixed-cationic intermediates in the cation exchange pathway from $[G\mathbf{1}]_{16}\cdot 4Na^+\cdot 4DNP^-$ to $[G\mathbf{1}]_{16}\cdot 4NH_4^+\cdot 4DNP^-$. The central Na^+, bound between the two symmetry-related G_8-Na^+ octamers, exchanges with either K^+ or NH_4^+ before the two outer Na^+ ions situated within the C_4 symmetric G_8 octamers. A structural rationale, based on differences in the cations' octahedral coordination geometries, is proposed to explain the differences in site exchange for these lipophilic G-quadruplexes. Large cations such as Cs^+ can be exchanged into the central cation binding site that holds the two symmetry-related C_4 symmetric G_8 octamer units together. The potential relevance of these findings to both supramolecular chemistry and DNA G-quadruplex structure are discussed.

Introduction

We describe efforts to understand how cation exchange occurs in supramolecular assemblies formed from G-quartets. The major aim of these studies is to learn how to use the G-quartet motif to build synthetic ion channels for ion transport across membranes.[1,2] Gellert and co-workers first described the G-quartet (Scheme 1) as the fundamental unit in the formation of hydrogels by 5′-GMP.[3] Pinnavaia and co-workers later showed that Na^+ and K^+ stabilize diastereomeric G_8-M^+ octamers by coordinating to the eight carbonyl oxygens of stacked G-quartets (Scheme 1).[4] Since those studies, many nucleosides, oligonucleotides, and synthetic derivatives have been shown to form G-quadruplex structures.[5] In the past decade, there has been an explosion in research on DNA and RNA G-quadruplexes, driven by their biological significance.[6] In supramolecular chemistry,

Scheme 1. G-Quartet Based Structures

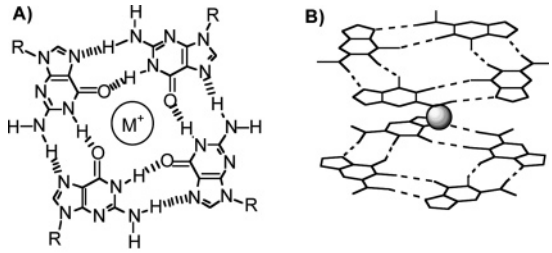

G-quartet assemblies have found use as gelators,[7] nanowires,[8] nanomachines,[9] and biosensors.[10] The G-quartet has also

(1) For recent reviews on synthetic ion channels, see: (a) Matile, S.; Som, A.; Sorde, N. *Tetrahedron* **2004**, *60*, 6405−6435. (b) Koert, U.; Al-Momani, L.; Pfeeifer, J. R. *Synthesis* **2004**, 1129−1146.
(2) For discussion of the ion channel nature of G-quadruplexes, see: (a) Chen, L.; Sakai, N.; Moshiri, S. T.; Matile, S. *Tetrahedron Lett.* **1998**, *39*, 3627. (b) Hud, N. V.; Schultze, P.; Sklenar, V.; Feigon, J. *J. Mol. Biol.* **1999**, *285*, 233. (c) Krishnan-Ghosh, Y.; Stephens, E.; Balasubramanian, S. *J. Am. Chem. Soc.* **2004**, *126*, 13895. (d) Datta, B.; Bier, M. E.; Roy, S.; Armitage, B. A. *J. Am. Chem. Soc.* **2005**, *127*, 4199.
(3) Gellert, M.; Lipsett, M.; Davies, D. *Proc. Natl. Acad. Sci. U.S.A.* **1962**, *48*, 2013−2018.
(4) (a) Pinnavaia, T. J.; Miles, H. T.; Becker, E. D. *J. Am. Chem. Soc.* **1975**, *97*, 7198−7200. (b) Pinnavaia, T.; Marshall, C.; Mettler, C.; Fisk, C.; Miles, H.; Becker, E. *J. Am. Chem. Soc.* **1978**, *100*, 3625−3627.
(5) For reviews on the G-quartet, see: (a) Guschlbauer, W.; Chantot, J. F.; Thiele, D. *J. Biomol. Struct. Dyn.* **1990**, *8*, 491−511. (b) Spada, G. P.; Gottarelli, G. *Synlett* **2004**, 596−602. (c) Davis, J. T. *Angew. Chem., Int. Ed.* **2004**, *43* (6), 668−698.
(6) For some recent reviews on the biological importance of G-quadruplexes, see: (a) Simonsson, T. *Biol. Chem.* **2001**, *382*, 621−628. (b) Neidle, S.; Parkinson, G. N. *Curr. Opin. Struct. Biol.* **2002**, *13*, 415−423.
(7) (a) Sreenivasachary, N.; Lehn, J.-M. *Proc. Natl. Acad. Sci. U.S.A.* **2005**, *102*, 5938−5943. (b) Ghoussoub, A.; Lehn, J.-M. *Chem. Commun.* **2005**, 5763−5766.
(8) (a) Sen, D; Gilbert, W. *Biochemistry* **1992**, *31*, 65−70. (b) Lu, M.; Guo, Q.; Kallenbach, N. R. *Biochemistry* **1992**, *31*, 2455−2459. (c) Marsh, T. C.; Henderson, E. *Biochemistry* **1994**, *33*, 10718−10724. (d) Marsh, T. C.; Vesenka, J.; Henderson, E. *Nucleic Acids Res.* **1995**, *23*, 696−700. (e) Marotta, S. P.; Tamburri, P. A.; Sheardy, R. D. *Biochemistry* **1996**, *35*, 10484−10492.
(9) (a) Li, J. W. J.; Tan, W. H. *Nano Lett.* **2002**, *2*, 315−318. (b) Alberti, P.; Mergny, J.-L. *Proc. Natl. Acad. Sci. U.S.A.* **2003**, *100*, 1569−1573. (c) Dittmer, W. U.; Reuter, A.; Simmel, F. C. *Angew. Chem., Int. Ed.* **2004**, *43*, 3350.
(10) (a) He, F.; Tang, Y.; Wang, S.; Li, Y.; Zhu, D. *J. Am. Chem. Soc.* **2005**, *127*, 12343−12346. (b) Nagatoishi, S.; Nojima, T.; Juskowiak, B.; Takenaka, S. *Angew. Chem., Int. Ed.* **2005**, *44*, 5067. (c) Ho, H. A.; Leclerc, M. *J. Am. Chem. Soc.* **2004**, *126*, 1384. (d) Nutiu, R.;. Li, Y. F. *J. Am. Chem. Soc.* **2003**, *125*, 4771. (e) Pavlov, V.; Xiao, Y.; Shlyahovsky, B.; Willner, I. *J. Am. Chem. Soc.* **2004**, *126*, 11768.

Scheme 2. Formation of Lipophilic G-Quadruplex from G **1**[a]

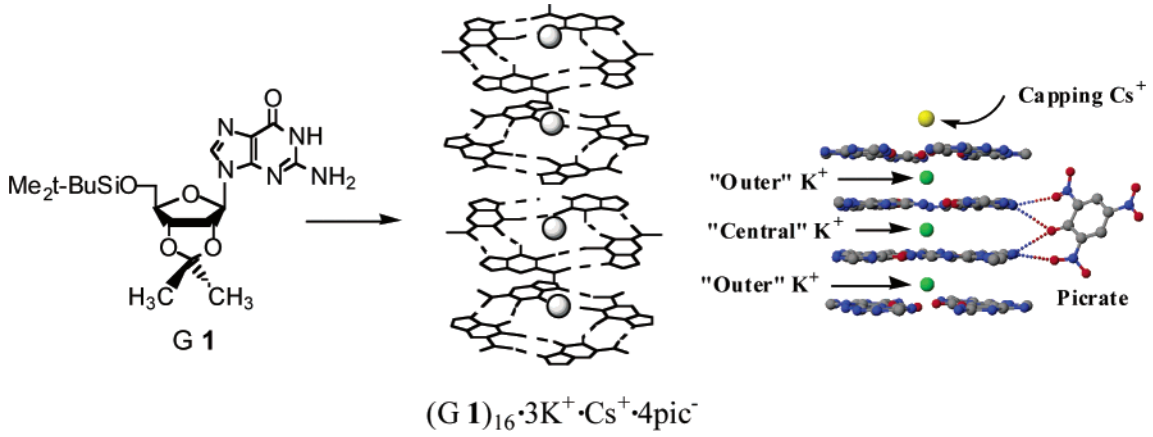

$$(G\,\mathbf{1})_{16}\cdot 3K^{+}\cdot Cs^{+}\cdot 4pic^{-}$$

[a] Picture on the right, from the crystal structure, shows the G-quartet layers, the four bound cations, and one of the four bound anions.

inspired synthesis of other hydrogen-bonded macrocycles with their own interesting structures and properties.[11]

We, and others, have been exploring the properties of lipophilic G-quadruplexes with an eye toward using them as self-assembled ionophores for selective sequestration of radioactive $^{137}Cs^{+}$ and $^{226}Ra^{2+}$[12,13] and as ion channels for transporting cations across lipid membranes.[14,15] To design such functional assemblies, it is imperative to understand their structural and dynamic properties. In the presence of cations, 5′-tert-butyldimethylsilyl-2′,3′-isopropylidene guanosine (G**1**) self-assembles into a lipophilic G-quadruplex $[G\mathbf{1}]_{16}\cdot 3K^{+}\cdot Cs^{+}\cdot 4pic^{-}$ (Scheme 2). A crystal structure shows the complex to be composed of four stacked G-quartets.[16] This pseudo-D_4 symmetric G-quadruplex can be described as a pair of head-to-tail, C_4 symmetric $[G\mathbf{1}]_8$ octamers that are coaxially stacked on one another in a head-to-head arrangement.[17] The two G_8 octamers use eight carbonyl oxygens to coordinate K^{+} in a square anti-prismatic geometry. A third K^{+}, with a nearly cubic coordination geometry, holds the two C_4 symmetric $[G\mathbf{1}]_8$ octamers together by binding to the two inner G-quartets.[17] A solvated Cs^{+} caps the G-quadruplex by sitting in a cavity above one of the outer G_4-quartets. This capping ion is dynamic in solution since the NMR spectra of the G-quadruplex shows only two sets of signals. If the capping ion was tightly bound, one would expect four sets of NMR signals for the four different G-quartet layers in $[G\mathbf{1}]_{16}\cdot 3K^{+}\cdot Cs^{+}\cdot 4pic^{-}$. The bound cations in these G-quadruplexes have been observed with ^{23}Na and ^{39}K solid-state NMR.[18,19] For ^{23}Na, all four channel ions (including the capping ion) were resolved.[18] Crystal structures and solution NMR also showed that four phenolate anions hydrogen bond to the two inner G-quartets.[16,20]

Since we aim to use these lipophilic G-quadruplexes as ion binders and transporters, we have been keen to understand their properties in solution. Recently, we used diffusion NMR to demonstrate that the hexadecameric $[G\mathbf{1}]_{16}\cdot 4K^{+}\cdot 4pic^{-}$, observed in the solid state, also predominates in organic solution.[21] We are also interested in the dynamics of G-quadruplex assembly and disassembly. The identity of both the bound anions and the bound cations significantly attenuate the kinetic stability of the G-quadruplex and modulate the rate of ligand exchange between G-quadruplex and monomer in solution.[20,22]

Recently, we have turned our attention to studying the cation exchange process within these lipophilic G-quadruplexes. In short, we would like to determine if the cations exchange through the ends of the G-quadruplex stack, much like an ion channel, or if cation exchange occurs through the sides of the G-quadruplex, especially since there is no covalent backbone connecting the different G-quartet layers. Both solution and solid-state NMR has provided much insight into the structure and dynamics of cation binding by DNA G-quadruplexes.[23−25] Pioneering studies by Feigon et al. used an $^{15}NH_4$ probe to identify different cation binding sites within the G-quadruplex formed by $d(G_4T_4G_4)_2$.[2b,26] On the basis of the exchange rates between solvated $^{15}NH_4$ and bound $^{15}NH_4$, they proposed that

(11) (a) Cai, M.; Marlow, A. L.; Fettinger, J. C.; Fabris, D.; Haverlock, T. J.; Moyer, B. A.; Davis, J. T. *Angew. Chem., Int. Ed.* **2000**, *39*, 1283−1285. (b) Fenniri, H.; Packiarajan, M.; Vidale, K. L.; Sherman, D. M.; Hallenga, K.; Wood, K. V.; Stowell, J. G. *J. Am. Chem. Soc.* **2001**, *123*, 3854−3855. (c) Sessler, J. L.; Sathiosatham, M.; Doerr, K.; Lynch, V.; Abboud, K. A. *Angew. Chem., Int. Ed.* **2000**, *39*, 1300−1303. (d) Sessler, J. L.; Jayawickramarajah, J.; Sathiosatham, M.; Sherman, C. L.; Brodbelt, J. S. *Org. Lett.* **2003**, *5*, 2627−2630. (e) Gubala, V.; Betancourt, J. E.; Rivera, J. M. *Org. Lett.* **2004**, *6*, 4735−4738. (d) Rakotondradany, F.; Palmer, A.; Toader, V.; Chen, B. Z.; Whitehead, M. A.; Sleiman, H. F. *Chem. Commun.* **2005**, 5441−5443.
(12) (a) Davis, J. T.; Tirumala, S. K.; Marlow, A. L. *J. Am. Chem. Soc.* **1997**, *119*, 5271−5272. (b) van Leeuwen, F.; Verboom, W.; Shi, X. D.; Davis, J. T.; Reinhoudt, D. N. *J. Am. Chem. Soc.* **2004**, *126*, 16575−12581. (c) van Leeuwen, F.; Miermans, C. J. H.; Beijleveld, H.; Tomasberger, T.; Davis, J. T.; Verboom, W.; Reinhoudt, D. N. *Environ. Sci. Technol.* **2005**, *39*, 5455−5459.
(13) (a) Gottarelli, G.; Masiero, S.; Spada, G. P. *J. Chem. Soc., Chem. Commun.* **1995**, 2555−2557. (b) Gubala, V.; De Jesus, D.; Rivera, J. M. *Tetrahedron. Lett.* **2006**, *47*, 1413−1416.
(14) Kaucher, M. S.; Harrell, W. A.; Davis, J. T. *J. Am. Chem. Soc.* **2006**, *128*, 38−39.
(15) Sakai, N.; Kamikawa, Y.; Nishii, M.; Matsuoka, T.; Kato, T.; Matile, S. *J. Am. Chem. Soc.* **2006**, *128*, 2218−2219.
(16) Forman, S. L.; Fettinger, J. C.; Pieraccini, S.; Gottarelli, G.; Davis, J. T. *J. Am. Chem. Soc.* **2000**, *122*, 4060−4067.
(17) A parallel-stranded DNA G-quadruplex shows similar dimerization and cubic coordination geometry in the solid state, see: Laughlan, G.; Murchie, A. I. H.; Norman, D. G.; Moore, M. H.; Moody, P. C. E.; Lilley, D. M. J.; Luisi, B. *Science* **1994**, *265*, 520−524.
(18) Wong, A.; Forman, S. L.; Fettinger, J. C.; Davis, J. T.; Wu, G. *J. Am. Chem. Soc.* **2002**, *124*, 742−743.
(19) Wu, G.; Wong, A.; Gan, Z.; Davis, J. T. *J. Am. Chem. Soc.* **2003**, *125*, 7182−7183.
(20) Shi, X. D.; Mullaugh, K. M.; Fettinger, J. C.; Jiang, Y.; Hofstadler, S. A.; Davis, J. T. *J. Am. Chem. Soc.* **2003**, *125*, 10830−10841.
(21) Kaucher, M. S.; Lam, Y. F.; Pierracini, S.; Gottarelli, G.; Davis, J. T. *Chem.—Eur. J.* **2005**, *11*, 164−173.
(22) Davis, J. T.; Kaucher, M. S.; Kotch, F. W.; Iezzi, M. A.; Clover, B. C.; Mullaugh, K. M. *Org. Lett.* **2004**, *6*, 4265−4268.
(23) Xu, Q. W.; Deng, H.; Braunlin, W. H. *Biochemistry* **1993**, *32*, 13130−13137.
(24) Basu, S.; Szewczak, A. A.; Cocco, M.; Strobel, S. A. *J. Am. Chem. Soc.* **2000**, *122*, 3240−3241.
(25) Wong, A.; Wu, G. *J. Am. Chem. Soc.* **2003**, *125*, 13895−13905.
(26) (a) Hud, N. V.; Schultze, P.; Feigon, J. *J. Am. Chem. Soc.* **1998**, *120*, 6403−6404. (b) Hud, N. V.; Schultze, P.; Hud, N. V.; Smith, F. W.; Feigon, J. *Nucleic Acids Res.* **1999**, *27*, 3018−3028.

cations flow through the ends of the DNA G-quadruplex pore, much like in an ion channel. Recently, Plavec and co-workers have also used $^{15}NH_4$ as a solution NMR probe to determine the rates of cation exchange within the G-quadruplex formed by $[d(G_3T_4G_3)]_2$.[27] They also have used ^{15}N NMR to identify the formation of mixed-dication intermediates in the $^{15}NH_4^+/K^+$ ion exchange process that occurs for $[d(G_3T_4G_3)]_2$.[28] Recent calculations have predicted that smaller ions such as Li^+ and Na^+ should move through the DNA G-quadruplex channels with relatively low activation barriers, when compared to the larger NH_4^+ and K^+ cations.[29]

In this paper, we are concerned with cation exchange in the lipophilic G-quadruplex $[G\mathbf{1}]_{16}\cdot 4Na^+\cdot 4DNP^-$ (where DNP is 2,6-dinitrophenolate). As previously mentioned, this hexadecamer has four cation binding sites in its solid-state structure: a capping site, two degenerate outer sites formed by the G_8-octamer units, and a central binding site located between the G_8-octamers. We studied cation exchange in solution using electrospray ionization mass spectrometry (ESI-MS) and NMR spectroscopy by adding cations with a stronger binding affinity (K^+ and NH_4^+) to an all-Na^+ G-quadruplex. The more favorable binding of K^+ or NH_4^+ to the G-quadruplex drove the K^+/Na^+ cation exchange. In this study, we aimed to (1) identify mixed-cation intermediates along the ion exchange pathway; (2) determine if different G-quadruplex binding sites have different affinities for cations; (3) identify a structural basis for any observed differences in the cation binding affinities; and (4) use this structural information to build new mixed-cationic G-quadruplexes.

Results and Discussion

Mass Spectrometry Shows Mixed-Cation G-Quadruplexes Formed by Sequential Ion Exchange. In general, G-quartets are stabilized by monovalent cations in the order $K^+ > NH_4^+ > Na^+ \gg Cs^+ > Li^+$.[5,25] Because of this difference in relative binding strength, the addition of a higher affinity cation to a G-quadruplex containing a weaker binding cation results in replacement of that initially bound ion. Such exchange has been amply demonstrated by solution ^1H NMR in water for Na^+/K^+ exchange in the hairpin G-quadruplex $d(G_3T_4G_3)_2$.[30] In that study, exchange between distinct cationic forms of the $d(G_3T_4G_3)_2$ G-quadruplexes was fast on the NMR chemical shift time scale, giving rise to a single, time-averaged set of signals. In our present case, the different cationic forms of the lipophilic G-quadruplex are in slow exchange on the chemical shift time scale, and what we hypothesized to be mixed-cation intermediates could be readily distinguished from the homomeric all-Na^+ and all-K^+ G-quadruplexes by solution ^1H NMR (see the following sections). In the DNA study, Feigon and colleagues demonstrated that the free energy of cation dehydration helped determine the relative binding affinity of different ions for DNA G-quartets in water. In an organic solvent, however, free cations are not hydrated, so there may be other factors that determine the cation's binding affinity for the G-quartet in an organic phase. Nonetheless, the mass spectrometric and solution NMR data, described next, indicate that G-quartets also have a higher affinity for K^+ over Na^+ in organic solvents such as CD_2Cl_2.

To unequivocally identify mixed-cation G-quadruplexes that form during the Na^+/K^+ ion exchange process, we first used electrospray ionization mass spectrometry (ESI-MS), a powerful method for characterizing noncovalent assemblies.[31] ESI-MS has been used to monitor the formation of G-quadruplexes by a variety of G-nucleosides and G-rich-oligonucleotides.[32,33] To the best of our knowledge, however, the Na^+/K^+ cation exchange process within a G-quadruplex has not been previously characterized by mass spectrometry. Thus, crystalline samples of $[G\mathbf{1}]_{16}\cdot 4\ Na^+\cdot 4DNP^-$ and $[G\mathbf{1}]_{16}\cdot 4\ K^+\cdot 4DNP^-$ were prepared according to standard procedures,[16,20] and their purity was confirmed by both NMR and mass spectrometry. ESI-MS analysis in the positive-ion mode showed distinct peaks for the intact Na^+ and K^+ G-quadruplexes at *m*/*z* 7435.3 and 7484.5, respectively (Figure 1a,e). These singly charged ions correspond to the molecular weight for the hexadecamer $[[G\mathbf{1}]_{16}\cdot 3M\cdot 2DNP]^+$, a species formed in the gas phase by losing one cation (presumably the weakly bound capping ion) and two DNP^- anions from the starting G-quadruplexes. As depicted in Figure 1b−d, we then monitored the cation exchange process by adding increasing amounts of KPh_4B to a solution of $[G\mathbf{1}]_{16}\cdot 4Na^+\cdot 4DNP^-$ in 1:1 CD_2Cl_2/CD_3CN. The major peaks in Figure 1b,c had *m*/*z* ratios intermediate between the two homomeric species, $[[G\mathbf{1}]_{16}\cdot 3Na\cdot 2DNP]^+$ and $[[G\mathbf{1}]_{16}\cdot 3K\cdot 2DNP]^+$. Significantly, the dominant molecular ion in each titration sample showed a 16 amu increase in mass, corresponding to the sequential displacement of a bound Na^+ by a single K^+ during the titration. For example, Figure 1b, corresponding to a sample containing 1 equiv of KPh_4B for each equiv of $[G\mathbf{1}]_{16}\cdot 4Na^+\cdot 4DNP^-$, showed a significant decrease in the $[[G\mathbf{1}]_{16}\cdot 3Na\cdot 2DNP]^+$ species (*m*/*z* 7435.3) with the concomitant formation of a new major species with *m*/*z* 7452.0. This new peak corresponds to a mixed-cation G-quadruplex of formula $[[G\mathbf{1}]_{16}\cdot K\cdot 2Na\cdot 2DNP]^+$. As depicted in Figure 1, there are two possible isomers for $[[G\mathbf{1}]_{16}\cdot K\cdot 2Na\cdot 2DNP]^+$, depending on whether one of the outer cations or the central cation is first replaced by K^+. The addition of a second equiv of KPh_4B led to the formation of $[[G\mathbf{1}]_{16}\cdot 2K\cdot Na\cdot 2DNP]^+$ (*m*/*z* 7468.2) as the dominant species in that region of the ESI mass spectrum (Figure 1c). Again, as depicted in Figure 1, there are two possible isomers for this second intermediate. Essentially complete conversion to the K^+ G-quadruplex (*m*/*z* 7484.5) occurred after the addition of just 4 equiv of KPh_4B to the solution of the Na^+ G-quadruplex (Figure 1d). The ESI-MS results depicted in Figure 1 are significant for the following reasons, as this data (1) confirm the pronounced K^+/Na^+ binding selectivity shown by this lipophilic G-quadruplex; (2) demon-

(27) Sket, P.; Crnugelj, M.; Kozminski, W.; Plavec, J. *Org. Biomol. Chem.* **2004**, *2*, 1970−1973.
(28) Sket, P.; Crnugelj, M.; Plavec, J. *Nucleic Acids Res.* **2005**, *33*, 3691−3697.
(29) van Mocrik, T.; Dingley, A. J. *Chem.−Eur. J.* **2005**, *11*, 6064−6079.
(30) Hud, N. V.; Smith, F. W.; Anet, F. A. L.; Feigon, J. *Biochemistry* **1996**, *35*, 15383−15390.
(31) For reviews, see: (a) Schalley, C. A. *Int. J. Mass. Spectrom.* **2000**, *194*, 11−39. (b) Schalley, C. A. *Mass Spectrom. Rev.* **2001**, *20*, 253−309.
(32) For ESI-MS studies on G-quadruplexes formed from mononucleosides and nucleotides, see: (a) Fukushima, K.; Iwahashi, H. *Chem. Commun.* **2000**, *11*, 895. (b) Manet, I.; Francini, L.; Masiero, S.; Pieraccini, S.; Spada, G. P.; Gottarelli, G. *Helv. Chim. Acta* **2001**, *84*, 2096. (c) Cai, M.; Shi, X.; Sidorov, V.; Fabris, D.; Lam, Y.-F.; Davis, J. T. *Tetrahedron* **2002**, *58*, 661−671. (d) Aggerholm, T.; Nanita, S. C.; Koch, K. J.; Cooks, R. G. *J. Mass. Spectrom.* **2003**, *38*, 87−97. (e) Baker, E. S.; Bernstein, S. L.; Bowers, M. T. *J. Am. Soc. Mass Spectrom.* **2005**, *16*, 989−997.
(33) For ESI-MS studies on G-quadruplexes formed from DNA and PNA, see: (a) Goodlett, D. R.; Camp, D. G., II; Hardin, C. C.; Corregan, M; Smith, R. D. *Biol. Mass Spectrom.* **1993**, *22*, 181. (b) Rosu, F.; Gabelica, V.; Houssier, C.; Colson, P.; De Pauw, E. *Rapid Commun. Mass Spectrom.* **2002**, *16*, 1729. (c) David, W. M.; Brodbelt, J.; Kerwin, S. M.; Thomas, P. W. *Anal. Chem.* **2002**, *74*, 2029−2033. (d) Vairamani, M.; Gross, M. L. *J. Am. Chem. Soc.* **2003**, *125*, 42. (e) Rosu, F.; Gabelica, V.; Shin-ya, K.; De Pauw, E. *Chem. Commun.* **2003**, 2702−2703.

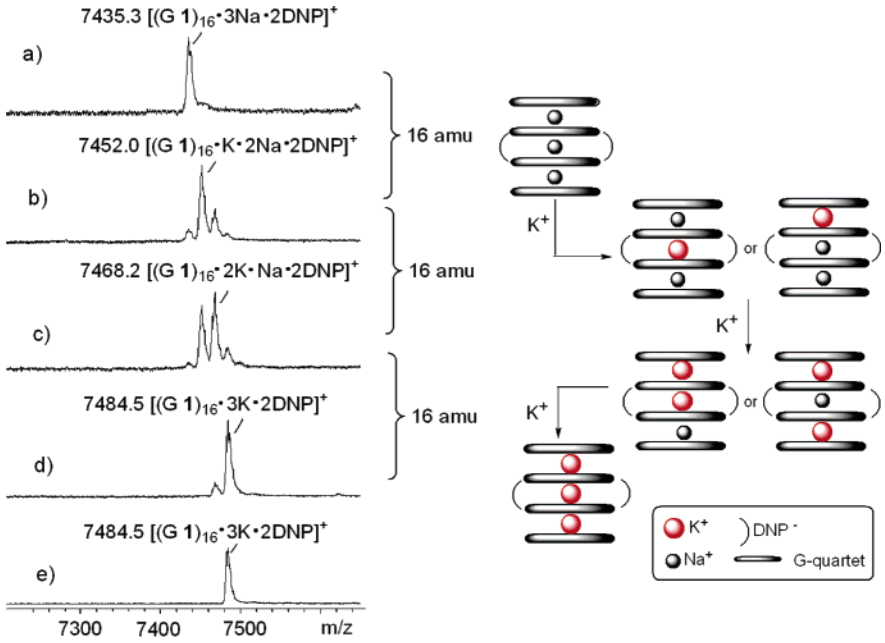

Figure 1. ESI-MS from titration of KPh_4B into a solution of $[G\mathbf{1}]_{16}\cdot 4Na^+\cdot 4DNP^-$ in 1:1 CD_2Cl_2/CD_3CN. (a) $[G\mathbf{1}]_{16}\cdot 4Na^+\cdot 4DNP^-$; (b) after addition of 1 equiv of KPh_4B; (c) after addition of 2 equiv of KPh_4B; (d) after addition of 4 equiv of KPh_4B; and (e) $[G\mathbf{1}]_{16}\cdot 4K^+\cdot 4DNP^-$. The diagram illustrates the possible mixed-cation G-quadruplexes that could be formed in the cation exchange process.

strate the formation of discrete mixed-cationic assemblies, such as $[[G\mathbf{1}]_{16}\cdot K\cdot 2Na\cdot 2DNP]^+$ and $[[G\mathbf{1}]_{16}\cdot 2K\cdot Na\cdot 2DNP]^+$, under conditions where substochiometric K^+ is present; and (3) illustrate the stepwise displacement of Na^+ cations by the stronger binding K^+ ion. This is the first time, to our knowledge, that mass spectrometric data have revealed the sequential ion exchange process in a G-quadruplex. Such ESI-MS titration experiments should also be informative for understanding the details of structure and ion binding in the rich array of DNA and RNA G-quadruplexes that have been discovered to date.

Proton NMR Indicates that the Central Na^+ Is the First Cation Exchanged for K^+ in Formation of Mixed Na^+, K^+ G-Quadruplexes. ESI-MS analysis of the titration of $[G\mathbf{1}]_{16}\cdot 4Na^+\cdot 4DNP^-$ with KPh_4B provided unequivocal evidence for the formation of the mixed Na^+, K^+ G-quadruplexes $[[G\mathbf{1}]_{16}\cdot K\cdot 2Na\cdot 2DNP]^+$ and $[[G\mathbf{1}]_{16}\cdot 2K\cdot Na\cdot 2DNP]^+$. However, the isomeric structures of these mixed G-quadruplexes, and the location of bound cations, could not be ascertained from the mass spectrometry data alone. For example, as shown in Figure 1, the first intermediate formed during Na^+/K^+ ion exchange could involve the replacement of either the outer or the central bound Na^+. In theory, these isomers should be distinguished by ^1H NMR based on their differences in symmetry. To identify the structures of these discrete intermediates, and to define specific cation exchange pathways, we turned to ^1H NMR spectroscopy, knowing that the chemical shifts of the G-quartet's amide N_1H protons are sensitive to the identity of the bound cation.[20,30] Figure 2a shows two distinct N_1H amide peaks for the all-Na^+ G-quadruplex $[G\mathbf{1}]_{16}\cdot 4Na^+\cdot 4DNP^-$ in 1:1 CD_2Cl_2/CD_3CN, with the signal at δ 11.46 ppm corresponding to the N_1H amide for the two inner G_4-quartets and the signal at δ 11.71 ppm due to the outer G_4-quartets.[20] In contrast, the G-quartet N_1H amide peaks for the K^+ G-quadruplex, $[G\mathbf{1}]_{16}\cdot 4K^+\cdot 4DNP^-$, occur at δ 11.35 (inner) and δ 11.58 ppm (outer), respectively (Figure 2g).

Figure 2b shows that two new amide N_1H signals (δ 11.42 and δ 11.75 ppm) appear after the addition of 0.5 equiv of KPh_4B to a solution of $[G\mathbf{1}]_{16}\cdot 4Na^+\cdot 4DNP^-$. These new N_1H signals are in slow exchange on the chemical shift time scale with signals for $[G\mathbf{1}]_{16}\cdot 4Na^+\cdot 4DNP^-$, a feature that helped us recognize this new species as a mixed Na^+, K^+ G-quadruplex. Further addition of KPh_4B (1 equiv) resulted in these new N_1H resonances becoming predominant, while the signals for $[G\mathbf{1}]_{16}\cdot 4Na^+\cdot 4DNP^-$ greatly diminished (Figure 2c). The new G-quadruplex in Figure 2c has only two N_1H signals (one set for the outer G-quartets and one set for the inner G-quartets), an indication that cation exchange occurred with the central Na^+ in $[G\mathbf{1}]_{16}\cdot 4Na^+\cdot 4DNP^-$ to give an intermediate with pseudo-D_4 symmetry, namely, $[[G\mathbf{1}]_{4(o)}\cdot Na^+\cdot[G\mathbf{1}]_{4(i)}\cdot K^+\cdot[G\mathbf{1}]_{4(i)}\cdot Na^+\cdot[G\mathbf{1}]_{4(o)}]$. If one of the outer Na^+ cations had been displaced by the first equiv of K^+, we would expect a lower symmetry hexadecamer, $[[G\mathbf{1}]_{4(o)}\cdot K^+\cdot[G\mathbf{1}]_{4(i)}\cdot Na^+\cdot[G\mathbf{1}]_{4(i)}\cdot Na^+\cdot[G\mathbf{1}]_{4(o)}]$, with four separate signals for its nonequivalent G-quartet layers.

Only after the addition of 2 equiv of KPh_4B did the ^1H NMR spectra show that the major G-quadruplex in solution had four new N_1H amide peaks of similar intensity, consistent with the formation of a mixed hexadecamer of lower symmetry, $[[G\mathbf{1}]_{4(o)}\cdot K^+\cdot[G\mathbf{1}]_{4(i)}\cdot K^+\cdot[G\mathbf{1}]_{4(i)}\cdot Na^+\cdot[G\mathbf{1}]_{4(o)}]$, where one of the two outer Na^+ cations must have been exchanged for a higher affinity K^+ (see the four labeled peaks in Figure 2d,e). Conversion into the all-K^+ G-quadruplex was essentially complete after the addition of just 4 equiv of KPh_4B (Figure 2f), a result that was consistent with the ESI-MS titration experiment (Figure 1).

Both ESI-MS and ^1H NMR titration data indicated that replacement of bound Na^+ by K^+ is a thermodynamically favorable process, particularly since the addition of only 4 equiv of KPh_4B led to essentially complete transformation of the all-Na^+ G-quadruplex to the all-K^+ G-quadruplex. In addition, mixed-cationic G-quadruplexes were detected in conversion of

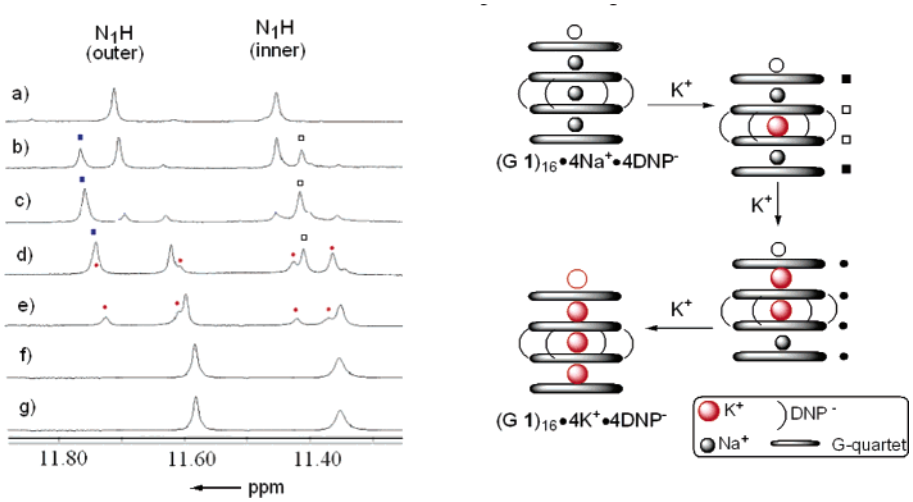

Figure 2. Region of the ^{1}H NMR spectra (400 MHz) showing the G-quartet NH1 amide protons during titration of $[G\mathbf{1}]_{16}\cdot 4Na^+\cdot 4DNP^-$ with KPh_4B in 1:1 CD_2Cl_2/CD_3CN. (a) $[G\mathbf{1}]_{16}\cdot 4Na^+\cdot 4DNP^-$. The mol ratio of added KPh_4B to the G-quadruplex, $[G\mathbf{1}]_{16}\cdot 4Na^+\cdot 4DNP^-$, is (b) 0.5:1; (c) 1:1; (d) 2:1; (e) 3:1; (f) 4:1; and (g) 12:1.

the all-Na^+ G-quadruplex to the all-K^+ G-quadruplex. Since Na^+ and K^+ are invisible using standard solution NMR spectroscopy,[34] we were not able to directly detect the different Na^+ and K^+ cations bound to various G-quadruplex species during the exchange process. To overcome this limitation, we used the NMR-active $^{15}NH_4^+$ as a surrogate for K^+ to identify the mixed-cation G-quadruplexes formed upon displacement of Na^+ by a higher affinity cation.

NMR Studies with $^{15}NH_4^+$ Confirm Identity of Mixed-Cationic G-Quadruplexes. The NH_4^+ cation has a similar coordination chemistry as K^+, and $^{15}NH_4^+$ has been used as an NMR probe to localize cations in DNA G-quadruplexes.[26−28] Wong and Wu have also used solid-state ^{23}Na NMR competition experiments to show that K^+ and NH_4^+ have similar free energies of binding to G-quadruplexes.[25] NMR titrations (Figure S1 in the Supporting Information) indicated that the order of the site exchange between free NH_4^+ and Na^+ bound to $[G\mathbf{1}]_{16}\cdot 4Na^+\cdot 4DNP^-$ was similar to that observed for the K^+/Na^+ exchange in Figure 1. Thus, mixed-cationic species that were in slow exchange with the all-Na^+ and all-NH_4^+ forms of the G-quadruplexes were identified by their separate sets of ^{1}H NMR signals. Both 2-D ^{15}N-^{1}H HSQC-ROESY[35] and ^{1}H-^{1}H NOESY data (Figure 3) for the all-NH_4^+ species $[G\mathbf{1}]_{16}\cdot 4NH_4^+\cdot 4DNP^-$ showed two types of bound $^{15}NH_4^+$, with one cation occupying the central location between the inner G-quartets and two $^{15}NH_4^+$ cations bound to the symmetry-related outer sites. The ^{15}N-^{1}H HSQC spectrum in Figure 3a shows two cross-peaks between the larger ^{15}N signal at δ 30.2 ppm and the larger ^{15}N-decoupled ^{1}H signal at δ 7.19 ppm. This correlation corresponds to the two $^{15}NH_4^+$ cations in the outer cation binding sites. The other cross-peak between the ^{15}N signal at δ 27.4 ppm and the ^{1}H signal at δ 7.30 ppm corresponds to $^{15}NH_4^+$ in the central binding site. These assignments were confirmed by NOESY (Figure 3b). NOE cross-peaks are observed between the two different $^{15}NH_4^+$ signals and the N_1H amide protons for the inner and outer G-quartets. The $^{15}NH_4^+$ cation bound in the central binding site shows cross-peaks only with the N_1H amide of the inner G-quartet (δ 11.41 ppm). In contrast, the stronger $^{15}NH_4^+$ signals show cross-peaks with N_1H amide protons for both the inner and the outer G-quartets, as would be expected for an ammonium cation bound between both types of layers. No $^{15}NH_4^+$ binding to the capping site was observed in these solution studies.[36]

The Na^+/K^+ exchange data in Figure 2 suggest that the central cation in $(G\mathbf{1})_{16}\cdot 4Na^+\cdot 4DNP^-$, which exchanges first, is bound less tightly than the outer cations coordinated within G_8-octamers. This hypothesis was supported by ^{15}N longitudinal relaxation measurements for the bound NH_4^+ cations in $[G\mathbf{1}]_{16}\cdot 4NH_4^+\cdot 4DNP^-$. Thus, ^{15}N T_1 spin−lattice relaxation times were found to be 12.5 s for the ^{15}N signal of the outer ions at δ 30.2 ppm and just 2.3 s for the central ion at δ 27.4 ppm. Although there are many factors that influence T_1 relaxation, the much shorter value for the centrally bound $^{15}NH_4^+$ may be because it is undergoing chemical exchange with solvated cations more readily than are the more tightly bound $^{15}NH_4^+$ cations in the two outer binding sites.[37]

Using $^{15}NH_4^+$ as a visible replacement ion for K^+, we performed a series of ^{15}N-filtered ^{1}H NMR experiments to unambiguously assign the two different cation binding sites within the G-quadruplex.[15] The ^{15}N-filtered and ^{15}N-decoupled ^{1}H NMR spectra in Figure 4 show the $^{15}NH_4^+/Na^+$ exchange that occurs upon titration of $^{15}NH_4Ph_4B$ into a solution of $[G\mathbf{1}]_{16}\cdot 4Na^+\cdot 4DNP^-$. The composition of mixed-cationic G-quadruplexes varies with added $^{15}NH_4^+$. After the addition of 1 equiv of $^{15}NH_4^+$ to $[G\mathbf{1}]_{16}\cdot 4Na^+\cdot 4DNP^-$ (Figure 4b), one resonance (δ 7.10 ppm) was observed in the ^{15}N-filtered ^{1}H NMR spectra, consistent with $^{15}NH_4^+$ being bound to a single site within the hexadecameric G-quadruplex. As the amount of

(34) Wu et al. have recently shown that solution ^{23}Na and ^{39}K NMR can be used for direct observations of alkali cations in G-quadruplexes: Wong, A.; Ida, R.; Wu, G. *Biochem. Biophys. Res. Commun.* **2005**, *337*, 363−366. While we saw a solution ^{23}Na NMR signal for $[G\mathbf{1}]_{16}\cdot 4Na^+\cdot 4DNP^-$, we could not resolve resonances for the separately bound Na^+ ions within this lipophilic G-quadruplex.

(35) Bodenhausen, G.; Ruben, D. J. *Chem. Phys. Lett.* **1980**, *69*, 185−189.

(36) An X-ray crystal structure of the all-NH_4^+ G-quadruplex $[G\mathbf{1}]_{16}\cdot 4NH_4^+\cdot 4DNP^-$ did not show any electron density for the capping ion. The other three NH_4^+ cations, all located in the central channel, were clearly visible in the structure. Iezzi, M.; Zavalij, P.; Davis, J. T., manuscript in preparation.

(37) For a discussion of the factors that influence N-15 T_1 values, see: Wei, A.; Raymond, M. K.; Roberts, J. D. *J. Am. Chem. Soc.* **1997**, *119*, 2915−2920.

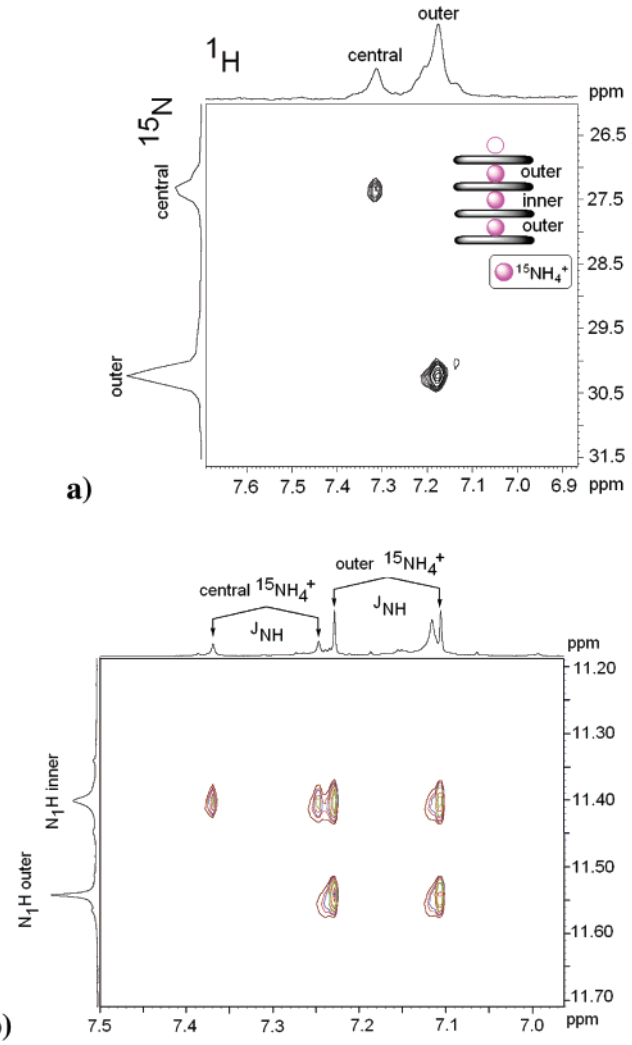

Figure 3. (a) Region from the 2-D ^{15}N-^{1}H HSQC-ROESY NMR spectrum of $[G\mathbf{1}]_{16}\cdot 4NH_4^+\cdot 4DNP^-$ in 1:1 CD_2Cl_2/CD_3CN showing cross-peaks between the ^{15}N NMR resonances and the ^{15}N-filtered ^{1}H resonances. (b) Region of the 2-D ^{1}H-^{1}H NOESY NMR spectra of $[G\mathbf{1}]_{16}\cdot 4NH_4^+\cdot 4DNP^-$ in 1:1 CD_2Cl_2/CD_3CN showing cross-peaks between the N_1H amide resonances and the ^{1}H resonances for the bound NH_4^+ cations. Both spectra were recorded on a 1 mM sample at 20 °C using a 500 MHz NMR spectrometer.

$^{15}NH_4^+$ increased, additional ^{15}N-decoupled signals for NH_4^+ resonances were observed, indicating further displacement of specific Na^+ ions by $^{15}NH_4^+$. The titration sample containing 12 equiv of $^{15}NH_4Ph_4B$ showed two $^{15}NH_4^+$ proton peaks (in a 1:2 ratio) at δ 7.31 ppm and δ 7.17 ppm, respectively (Figure 4f). This pattern is consistent with the structure of the all-NH_4^+ G-quadruplex $(G\mathbf{1})_{16}\cdot 4^{15}NH_4^+\cdot 4DNP^-$ (Figure 4g). The other two equal intensity $^{15}NH_4^+$ signals that appear and then disappear during the course of the titration (marked by blue circles in Figure 4c−f) are due to a G-quadruplex that contains two bound $^{15}NH_4^+$ cations and one bound Na^+ cation, namely, $[[G\mathbf{1}]_{4(o)}\cdot{}^{15}NH_4^+\cdot[G\mathbf{1}]_{4(i)}\cdot{}^{15}NH_4^+\cdot[G\mathbf{1}]_{4(i)}\cdot Na^+\cdot[G\mathbf{1}]_{4(o)}]$.

We reasoned that the species formed in Figure 4b, after the addition of 1 equiv of $^{15}NH_4Ph_4B$ to $[G\mathbf{1}]_{16}\cdot 4Na^+\cdot 4DNP^-$, must be a D_4 symmetric mixed G-quadruplex, with the $^{15}NH_4^+$ cation bound in the central cavity between two G_8-Na^+-octamers. This assignment for the species $[[G\mathbf{1}]_{4(o)}\cdot Na^+\cdot[G\mathbf{1}]_{4(i)}\cdot{}^{15}NH_4^+\cdot[G\mathbf{1}]_{4(i)}\cdot Na^+\cdot[G\mathbf{1}]_{4(o)}]$ was confirmed by a 2-D ^{1}H, ^{1}H NOESY experiment. Figure 5 shows a cross-peak between the $^{15}NH_4^+$ protons centered at δ 7.10 ppm and the N_1H protons of the inner G-quartet layers at δ 11.40 ppm. In marked contrast, there were no ^{1}H ^{1}H NOEs between this bound $^{15}NH_4^+$ and the N_1H amide of the outer G-quartet layers at δ 11.79 ppm.

The NMR data in Figures 4 and 5 conclusively demonstrate that the initial NH_4^+/Na^+ cation exchange occurs between solvated $^{15}NH_4^+$ and the centrally bound D_4 symmetric Na^+ cation to give $[[G\mathbf{1}]_{4(o)}\cdot Na^+\cdot[G\mathbf{1}]_{4(i)}\cdot{}^{15}NH_4^+\cdot[G\mathbf{1}]_{4(i)}\cdot Na^+\cdot[G\mathbf{1}]_{4(o)}]$ as the first discrete intermediate in the cation exchange process. A battery of 1-D selective NOE experiments (Figure S2 in the Supporting Information) confirmed that the addition of more than 1 equiv of $^{15}NH_4Ph_4B$ results in the displacement of an outer Na^+ cation to give the mixed 2:1 NH_4^+/Na^+ species, $[[G\mathbf{1}]_{4(o)}\cdot{}^{15}NH_4^+\cdot[G\mathbf{1}]_{4(i)}\cdot{}^{15}NH_4^+\cdot[G\mathbf{1}]_{4(i)}\cdot Na^+\cdot[G\mathbf{1}]_{4(o)}]$ (blue circles in Figure 4c−f).

Cation Exchange Pathway in the Lipophilic G-Quadruplex. Firm identification of these mixed-cationic G-quadruplexes, using the combined ESI-MS and ^{1}H, ^{15}N NMR data, allowed us to define a pathway for exchange of monovalent cations in this lipophilic G-quadruplex (Scheme 3). Thus, higher affinity cations such as K^+ and NH_4^+ preferentially displace the central Na^+ cation in the G-quadruplex $[G\mathbf{1}]_{16}\cdot 4Na^+\cdot 4DNP^-$ to give the pseudo-D_4 symmetric mixed-cation G-quadruplex $[[G\mathbf{1}]_{4(o)}\cdot Na^+\cdot[G\mathbf{1}]_{4(i)}\cdot{}^{15}NH_4^+\cdot[G\mathbf{1}]_{4(i)}\cdot Na^+\cdot[G\mathbf{1}]_{4(o)}]$ as the first intermediate. Consequently, sequential exchange of the two tighter-bound outer cations finish the ion exchange process. Control experiments, where components were mixed in the appropriate ratios, confirmed that the process depicted in Scheme 3 is under complete thermodynamic control (data not shown).

Why is it easier to displace the central Na^+ ion in $[G\mathbf{1}]_{16}\cdot 4Na^+\cdot 4DNP^-$, as opposed to the ions in the outer binding sites of the G-quadruplex? We propose that differences in the cations' octahedral coordination geometries at these separate binding sites is responsible for the relative facility of cation exchange. Crystal structures for the $[\mathbf{1}]_{16}\cdot 4M^+\cdot 4A^-$ system show that the central cation in this hexadecameric assembly has an almost cubic coordination geometry with the eight oxygen atoms of the two inner G-quartets.[16,20] In contrast, the oxygen ligands that sandwich the outer Na^+ cations are twisted more toward a square anti-prismatic coordination geometry. Cubic coordination geometry is relatively rare because of the electrostatic repulsion that occurs between the ligand atoms that eclipse each other.[38,39] The anti-prismatic geometry, on the other hand, is usually more favorable since the ligand atoms are twisted, so as to minimize ligand−ligand contacts while maintaining an optimum ligand−M^+ distance.[38,39] This influence of coordination geometry on the interaction energy of cations within G_8−M^+ octamers has been addressed recently by Meyer and co-workers using DFT calculations.[40] They found that a G_8−Na^+ octamer with square anti-prismatic coordination was more stable (by about 9 kcal/mol) than a G_8−Na^+ octamer with a cubic coordination environment. We propose that, because of these differences in coordination geometry in $[G\mathbf{1}]_{16}\cdot 4Na^+\cdot 4DNP^-$, the central cation is bound less strongly than are the outer cations and, therefore, exchanges more readily with the higher affinity K^+

(38) (a) Cotton, F. A.; Wilkinson, G. *Advanced Inorganic Chemistry*; Wiley and Sons, New York, 1980. (b) Al-Karaghouli, A. R.; Day, R. O.; Wood, J. S. *Inorg. Chem.* **1978**, *17*, 3702−3706.
(39) Psillakis, E.; Jeffery, J. C.; McCleverty, J. A.; Ward, M. D. *Chem. Commun.* **1997**, 1965−1966.
(40) Meyer, M.; Hocquet, A.; Suhnel, J. *J. Comput. Chem.* **2005**, *26*, 352−364.

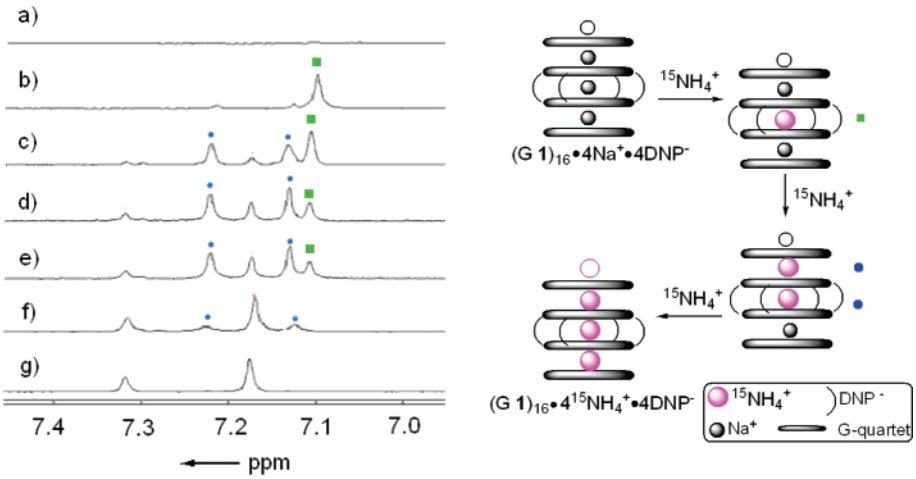

Figure 4. ^{15}N-filtered ^1H NMR (500 MHz) spectra of $^{15}NH_4Ph_4B$ titration the solution of $[G\mathbf{1}]_{16}\cdot 4Na^+\cdot 4DNP^-$ in 1:1 CD_2Cl_2/CD_3CN with mol ratio at (a) 0:1; (b) 1:1; (c) 2:1; (d) 3:1; (e) 4:1; (f) 12:1; and (g) $[G\mathbf{1}]_{16}\cdot 4^{15}NH_4^+\cdot 4DNP^-$.

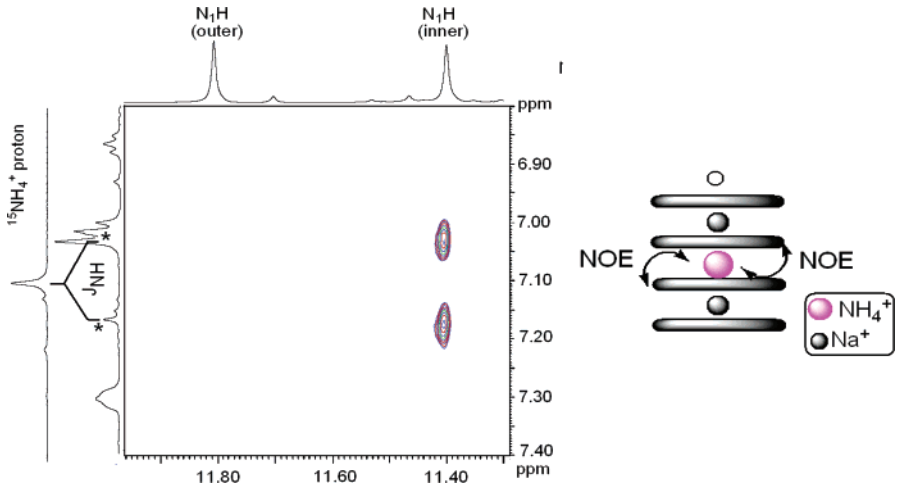

Figure 5. Portion of a NOESY spectrum of a 1:1 $^{15}NH_4$ Ph_4B titration into $[G\mathbf{1}]_{16}\cdot 4Na^+\cdot 4DNP^-$ in 1:1 CD_2Cl_2/CD_3CN. The 2-D spectrum shows the NOE cross-peak between the $^{15}NH_4^+$ ^1H resonance with the N_1H of the inner G-quartet layer. The chemical shifts of δ 11.79 and 11.40 ppm correspond to the N_1H amide protons for the outer and inner G-quartet layers. The chemical shift of the $^{15}NH_4^+$ proton was confirmed from the ^{15}N decoupled ^1H NMR spectrum showing a single peak at δ 7.10 ppm.

Scheme 3. Proposed Central Insertion Pathway for Cation Exchange in This Lipophilic G-Quadruplex System

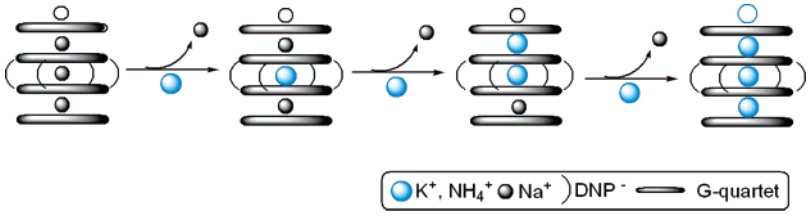

or NH_4^+. Indeed, X-ray data show that the separation between the two inner G-quartets is greater than the average separation between the inner and the outer G-quartet layers. There is more space in the central ion binding site than in the outer sites.

This central cation may serve to help dimerize discrete G_8-M^+ octamer units into more highly ordered superstructures. Indeed, we have previously shown for another lipophilic G-quadruplex that the K^+ ion concentration can influence the degree of self-association.[21] Thus, at low K^+ concentrations, 5′-(3,5-bis(methoxy)benzoyl)-2′,3′-isopropylidene (G**2**) forms an octamer. Upon the addition of extra K^+, these $[G\mathbf{2}]_8\cdot K^+$ octamers dimerize to form a stable $[G\mathbf{2}]_{16}$-hexadecamer in solution. A similar phenomenon has been seen for the tetrahymena telomere sequence d(T_2G_4) and for the human telomere sequence d(TTAGGG), which are both monomeric G-quadruplexes at lower K^+ ion concentrations but form head-to-head G-quadruplex dimers at higher K^+ ion concentrations.[41]

Larger Cs^+ cation, But Not Smaller Li^+, Can Displace the Central Cation in the Na^+ G-Quadruplex. The final experiments in this study were based on the hypothesis that the near cubic coordination geometry for the central cation binding site should accommodate a larger cation much more readily than a smaller cation. We reasoned that a larger cation should maximize the separation between the eclipsing oxygen atoms

(41) (a) Wang, Y.; Patel, D. J. *Biochemistry* **1992**, *31*, 8112−8119. (b) Kato, Y.; Ohyama, T.; Mita, H.; Yamamoto, Y. *J. Am. Chem. Soc.* **2005**, *127*, 9980−9981. (c) Balagurumoorthy, P.; Brahmachari, S. *J. Biol. Chem.* **1994**, *269*, 21858−21869.

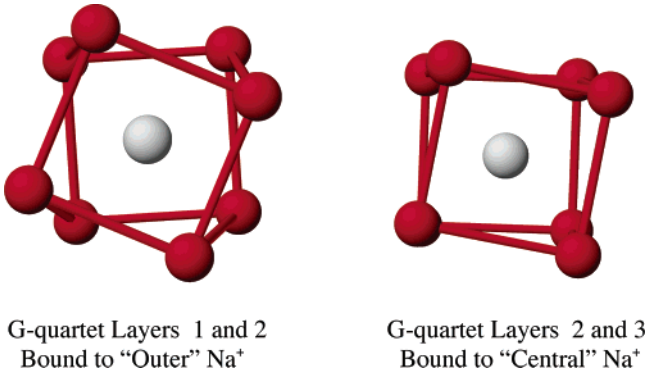

Figure 6. These depictions are taken from the crystal structure for $[G\mathbf{1}]_{16}\cdot 4Na^{+}\cdot 4pic^{-}$ (ref 16). The illustrations show the octahedral coordination geometry for one of the outer Na^{+} cations (on the left) and for the central Na^{+} (right). The central Na^{+} has an almost cubic coordination geometry, whereas the oxygen ligands are twisted toward the energetically more favorable square anti-prism geometry for the outer Na^{+}.

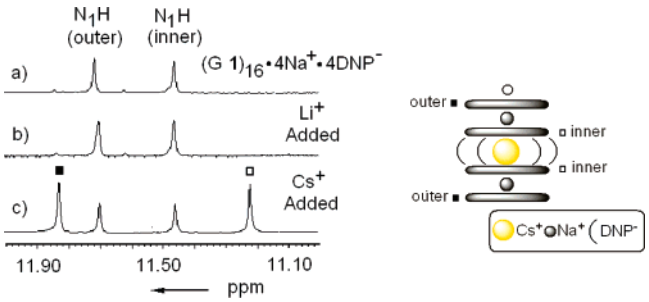

Figure 7. ^{1}H NMR spectra of N_1H region of different G-quadruplex solutions in CD_2Cl_2/CD_3CN at 20 °C. (a) $[G\mathbf{1}]_{16}\cdot 4Na^{+}\cdot 4DNP^{-}$; (b) 10:1 mol ratio of $LiPh_4B$ and $[G\mathbf{1}]_{16}\cdot 4Na^{+}\cdot 4DNP^{-}$; (c) 8:1 mol ratio of CsPh4B; and $[G\mathbf{1}]_{16}\cdot 4Na^{+}\cdot 4DNP^{-}$.

within the central ion binding site. As shown in Figure 7c, this hypothesis appears reasonable, as we could substitute this position with Cs^{+} ($r = 1.67$ A), a large cation that typically is not thought to stabilize G_8-octamers. Thus, the addition of 8 equiv of $CsPh_4B$ to a solution of the Na^{+} G-quadruplex led to the telltale formation of two new G-quartet N_1H amide signals, consistent with displacement of the central Na^{+} cation and formation of a pseudo-D_4 symmetric G-quadruplex $[[\mathbf{G}1]_{4(o)}\cdot Na^{+}\cdot[\mathbf{G}1]_{4(i)}\cdot Cs^{+}\cdot[\mathbf{G}1]_{4(i)}\cdot Na^{+}\cdot[\mathbf{G}1]_{4(o)}]$. In marked contrast, the addition of 10 equiv of $LiPh_4B$ to the same Na^{+} G-quadruplex gave no noticeable formation of any mixed-cationic species. Thus, unlike Cs^{+} ($r = 1.67$ A), the smaller Li^{+} ($r = 0.59$ A) does not displace Na^{+} ($r = 0.97$ A) from the central ion binding site in this G-quadruplex. These experiments show that new, mixed-cationic G-quadruplexes can be rationally prepared based on the combined structural information from X-ray crystallography, ESI mass spectrometry, and solution NMR spectroscopy. These results also suggest that large ions such as Cs^{+} may well stabilize higher ordered DNA G-quadruplexes that are capable of forming head-to-head dimers with a cubic coordination geometry.[17,41]

Conclusion

In summary, we have studied the cation exchange between competitive cations in solution and Na^{+} ions bound to the lipophilic G-quadruplex $[G\mathbf{1}]_{16}\cdot 4Na^{+}\cdot 4DNP^{-}$. Cations with a stronger binding affinity for G-quadruplexes, such as K^{+}, drive the cation exchange process. Both ESI-MS and NMR measurements of the K^{+} titration into $[G\mathbf{1}]_{16}\cdot 4Na^{+}\cdot 4DNP^{-}$ revealed that cation exchange is a sequential process, as discrete mixed-cation intermediates were detected. Using the $^{15}NH_4^{+}$ cation as a probe, the identity of these mixed-cation G-quadruplex isomers was determined by ^{15}N-filtered ^{1}H NMR, NOESY, and selective NOE experiments. A central insertion pathway, in which free cations first replace the central cation in $[G\mathbf{1}]_{16}\cdot 4Na^{+}\cdot 4DNP^{-}$, is operative in this lipophilic G-quadruplex. A structural rationale, based on the different solid-state octahedral coordination geometries in $[G\mathbf{1}]_{16}\cdot 4Na^{+}\cdot 4DNP^{-}$, was proposed to explain the differences in site exchange between the central and the outer binding sites for these lipophilic G-quadruplexes.

The strategy that we have outlined in this paper may also be useful for identification of specific ion exchange pathways in G-quadruplexes formed by DNA and RNA oligonucleotides, particularly for those systems that have been shown to form dimeric G-quadruplexes either in the solid-state or in solution. Finally, these mechanistic studies on cation exchange, which clearly couple aspects of the crystal structure to solution state properties, should help us better understand the factors that control assembly and disassembly of lipophilic G-quadruplexes. Such knowledge will guide our future efforts to build selective ionophores and synthetic ion channels. For example, unlike in DNA G-quadruplexes,[2b,26] the cations in these lipophilic G-quadruplexes apparently do not move through the ends of the central channel. In fact, the cation in the middle of the assembly is the easiest to displace. Thus, it is likely that covalent sidechains will be needed to link together lipophilic G-units so as to generate an appropriate building block for a synthetic ion channel. Such covalent linkages should stabilize the center of G-quadruplex structures. One attractive design for a transmembrane G-quadruplex channel, proposed by Armitage,[2d] is a G-rich PNA strand. Such precursors, as well as post-assembly modifications of lipophilic G-quadruplexes,[14] are currently being explored in our lab.

Experimental Procedures

General Method. ^{1}H NMR spectra were recorded on a Bruker Avance 400 instrument operating at 400 MHz or on a Bruker DRX-500 instrument operating at 500 MHz. Chemical shifts are reported in ppm relative to the residual protonated solvent peak. Electrospray ionization mass spectra were recorded on a Jeol AccuTOF mass spectrometer using electrospray ionization techniques. Deuterated solvents were purchased from Cambridge Isotope Laboratories. All chemicals and solvents were purchased from Sigma, Fluka, Aldrich, or Acros. G**1**;[16] the lipophilic G-quadruplexes ($[G\mathbf{1}]_{16}\cdot 4K^{+}\cdot 4DNP^{-}$, $[G\mathbf{1}]_{16}\cdot 4Na^{+}\cdot 4DNP^{-}$, and $[G\mathbf{1}]_{16}\cdot 4^{15}NH_4^{+}\cdot 4DNP^{-}$);[20] the potassium and sodium 2,6-dinitrophenolates;[20] and the ammonium (^{15}N) tetraphenylborate[42] were all prepared following published methods.

ESI-MS Spectrometry. The ESI-MS experiments were performed using the positive ionization mode on a Jeol AccuTOF mass spectrometer. The G-quadruplex solutions (~71 μM) in 1:1 CD_2Cl_2/CD_3CN were infused by a syringe pump into the mass spectrometer at a flow rate of 4 μL/min. The needle voltage was tuned to 2 to ~3 kV, and the orifice 1 voltage was set to 200 to ~250 V to obtain maximum sensitivity. The temperature for both the desolvation chamber and for orifice 1 was set to 30 °C. Spectra were acquired over a m/z range of 7000−8100.

NMR Titrations. A stock solution of $[G\mathbf{1}]_{16}\cdot 4Na^{+}\cdot 4DNP^{-}$ (2 mL) was prepared at a concentration of 3.57 mM in CD_2Cl_2, and 2 mL of a cation solution (KPh_4B and $^{15}NH_4Ph_4B$) in a range of 17.8−35.7 mM

(42) Andersen, E. K.; Andersen, I. G. K.; Ploud-Sorensen, G. *Acta. Chem. Scand.* **1989**, *43*, 624−635.

was prepared in CD_3CN. Equal amounts of the solution of $[G\mathbf{1}]_{16}\cdot 4Na^+\cdot 4DNP^-$ (200 μL) were loaded into six 5 mm NMR tubes. An increasing amount of salt solution (from 10 to 24 μL) was added in aliquots to the NMR sample tubes, giving mixtures containing the following mol ratios of $[G\mathbf{1}]_{16}\cdot 4Na^+\cdot 4DNP^-$ to KPh_4B: 1:0, 1:0.5, 1:1, 1:2, 1:3, and 1:4. Extra solvent was added to the NMR tubes to make sure the titration samples were 1:1 CD_2Cl_2/CD_3CN. A constant volume of 500 μL was used for each titration sample, so that the concentration of $[G\mathbf{1}]_{16}\cdot 4Na^+\cdot 4DNP^-$ remained constant. The NMR spectra were recorded 15 min after each titration and also 6 h later to ensure that equilibrium has been achieved in the cation exchange reactions.

^{15}N-Filtered ^{1}H NMR Experiment. The ^{15}N-filtered ^{1}H NMR experiments, carried out by titration of $^{15}NH_4Ph_4B$ into a solution of $[G\mathbf{1}]_{16}\cdot 4Na^+\cdot 4DNP^-$ in 1:1 CD_2Cl_2/CD_3CN, were recorded at 298 K using the 1-D HSQC pulse sequence.[35] The experiments were conducted in the phase-sensitive mode using the echo/anti-echo TPPT gradient selection method. The relaxation delay was 8.0 s. The spectra were taken with a sweep of 16.0 ppm. A total of 48 scans were acquired for each sample during the data collection.

NOESY Experiment. The NOESY experiments carried out after ion exchange had occurred for a sample containing equimolar $^{15}NH_4Ph_4B$ and $[G\mathbf{1}]_{16}\cdot 4Na^+\cdot 4DNP$ in 1:1 CD_2Cl_2/CD_3CN were recorded at 298 K using the NOESY pulse sequence.[43] The experiments were conducted in the phase sensitive mode using the TPPI method. The relaxation delay was 2.5 s, and the mixing time was 500 ms. The spectral width was 8012 Hz in each dimension. A total of 48 scans were collected for each time increment. A total of 512 serial files were collected, resulting in a data matrix of 512 × 2048.

Selective NOE Experiment. The selective NOE experiments carried out after ion exchange had occurred for a sample containing 2 molar equiv of $^{15}NH_4Ph_4B$ and 1 equiv of $[G\mathbf{1}]_{16}\cdot 4Na^+\cdot 4DNP$ in 1:1 CD_2Cl_2/CD_3CN were recorded at 298 K with the 1-D NOE pulse sequence.[44] The experiments were conducted using a selective inversion pulse on the peak of interest. The relaxation delay was 5.0 s, and mixing time was 500 ms. The spectra were taken with a sweep of 16.0 ppm. A total of 1600 scans were applied for the data collection.

Acknowledgment. We thank the Department of Energy (BES, Separations and Analysis Program) for financial support. M.I. thanks the University of Maryland's HHMI program for an undergraduate fellowship.

Supporting Information Available: Experimental protocols and selected spectroscopic data. This material is available free of charge via the Internet at http://pubs.acs.org.

JA064878N

(43) Wagner, R.; Berger, S. *J. Magn. Reson.* **1996**, *123*, 119−121.

(44) Stott, K.; Stonehouse, J.; Keeler, J.; Hwang, T. L.; Shaka, A. J. *J. Am. Chem. Soc.* **1995**, *117*, 4199−4200.